

SUPPORTING INFORMATION

Hydrogen production from formic acid decomposition in the liquid phase using Pd nanoparticles supported on CNFs with different surface properties

Felipe Sanchez,^a Mohammad Hayal Alotaibi,^b Davide Motta,^a Carine Edith Chan-Thaw,^c Andrianelison Rakotomahevitra,^c Tommaso Tabanelli,^d Alberto Roldan,^{a*} Ceri Hammond,^a Qian He,^a Tom Davies,^a Alberto Villa^{*e} and Nikolaos Dimitratos^{*a}

^aCardiff Catalysis Institute, School of Chemistry, Cardiff University, Main Building, Park Place, Cardiff, CF10 3AT, UK

^bJoint Center of Excellence in Integrated Nano-Systems, King Abdulaziz City for Science and Technology, P.O. Box 6086 Riyadh 11442 Saudi Arabia

^cInstitut pour la Maîtrise de l'Énergie – Université d'Antananarivo BP 566, 101 Antananarivo, Madagascar

^dDipartimento di Chimica Industriale "Toso Montanari", Alma Mater Studiorum Università di Bologna, Viale Risorgimento 4, 40136 Bologna, Italy

^eDipartimento di Chimica, Università degli studi di Milano, via Golgi 19, 20133, Milano, Italy

* corresponding and co-corresponding authors

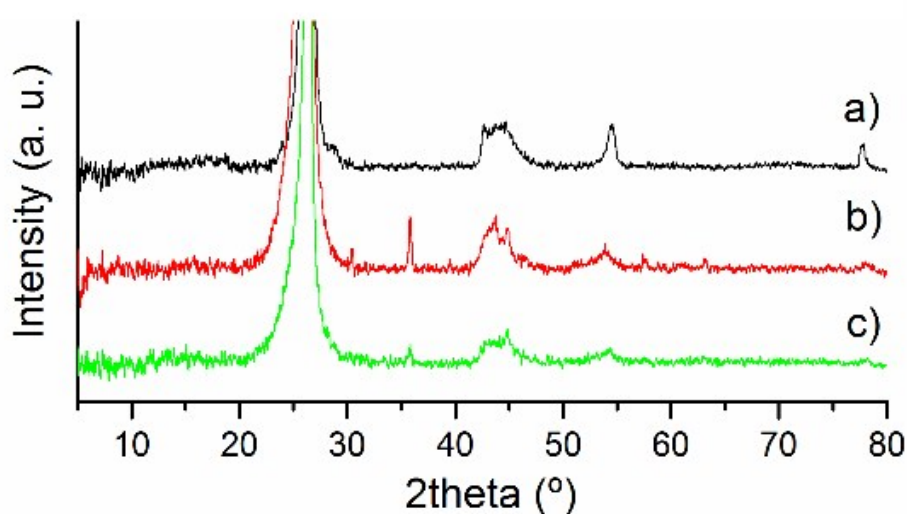


Figure S1. XRD patterns of the supports. (a) CNF-HHT, (b) CNF-LHT, (c) CNF-PS.

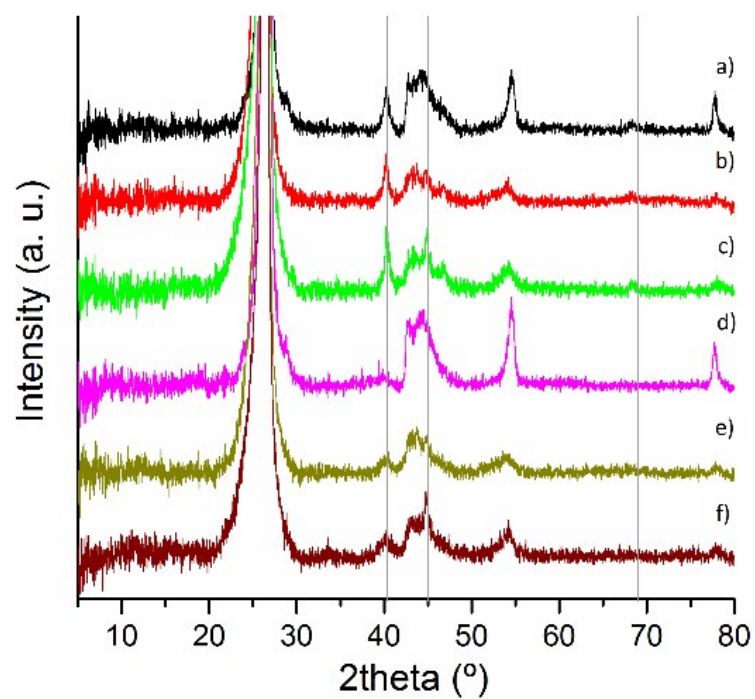


Figure S2. XRD patterns of used Pd/CNF (a) Pd_{IMP}/CNF-HHT, (b) Pd_{IMP}/CNF-LHT, (c) Pd_{IMP}/CNF-PS, (d) Pd_{SI}/CNF-HHT, (e) Pd_{SI}/CNF-LHT, (f) Pd_{SI}/CNF-PS.

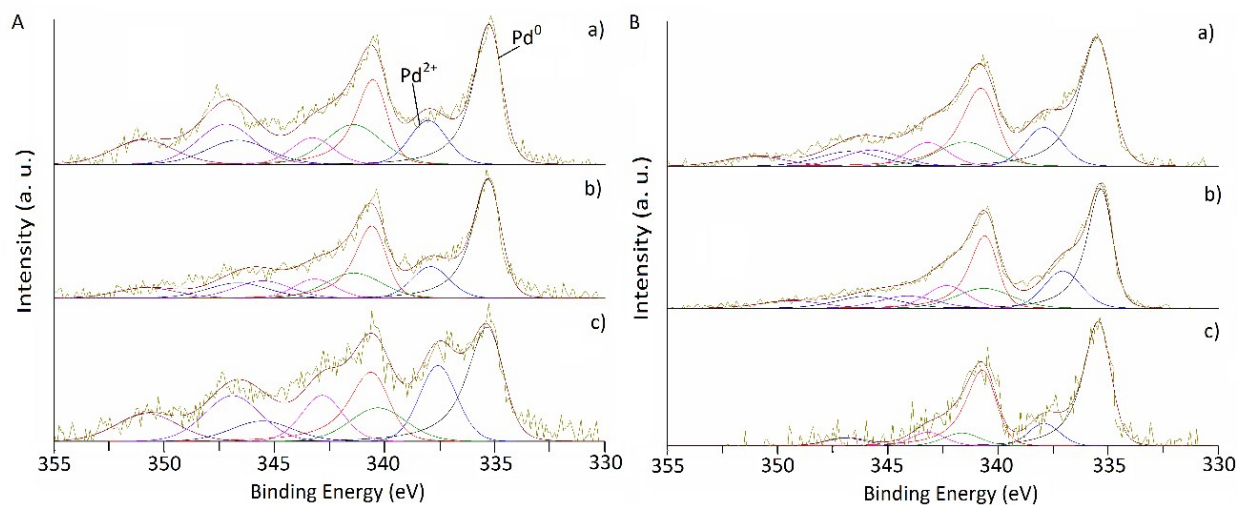


Figure S3. XPS spectra of used Pd/CNF (A) Catalyst synthesised by impregnation: (a) $\text{Pd}_{\text{IMP}}/\text{CNF-HHT}$, (b) $\text{Pd}_{\text{IMP}}/\text{CNF-LHT}$, (c) $\text{Pd}_{\text{IMP}}/\text{CNF-PS}$. (B) Catalysts synthesised by sol-immobilisation: (a) $\text{Pd}_{\text{SI}}/\text{CNF-HHT}$, (b) $\text{Pd}_{\text{SI}}/\text{CNF-LHT}$, (c) $\text{Pd}_{\text{SI}}/\text{CNF-PS}$.

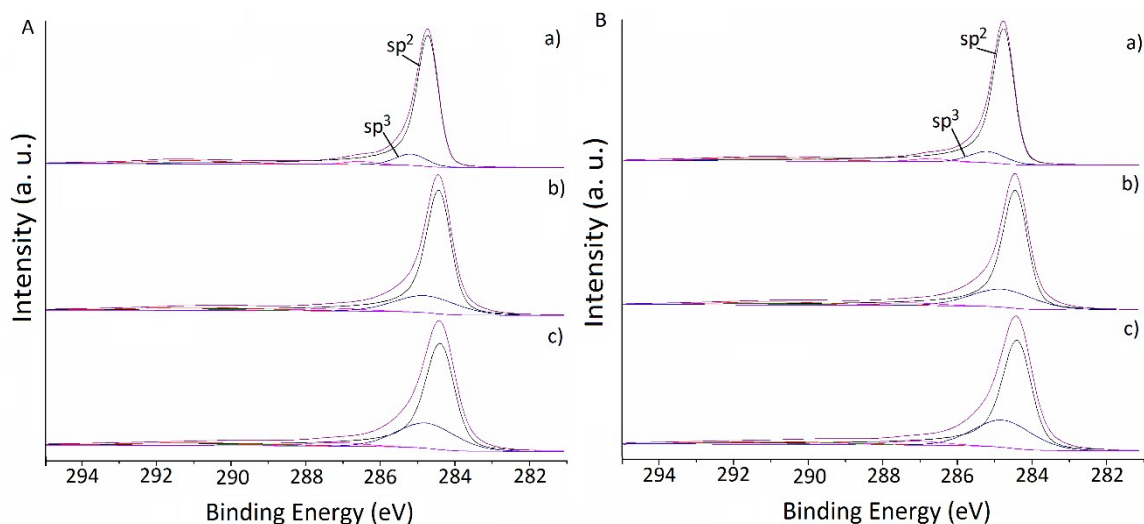


Figure S4. XPS spectra of fresh Pd/CNF in the binding energy region of 281–295 eV corresponding to C1s. (A) Catalyst synthesised by impregnation: (a) $\text{Pd}_{\text{IMP}}/\text{CNF-HHT}$, (b) $\text{Pd}_{\text{IMP}}/\text{CNF-LHT}$, (c) $\text{Pd}_{\text{IMP}}/\text{CNF-PS}$. (B) Catalysts synthesised by sol-immobilisation: (a) $\text{Pd}_{\text{SI}}/\text{CNF-HHT}$, (b) $\text{Pd}_{\text{SI}}/\text{CNF-LHT}$, (c) $\text{Pd}_{\text{SI}}/\text{CNF-PS}$.

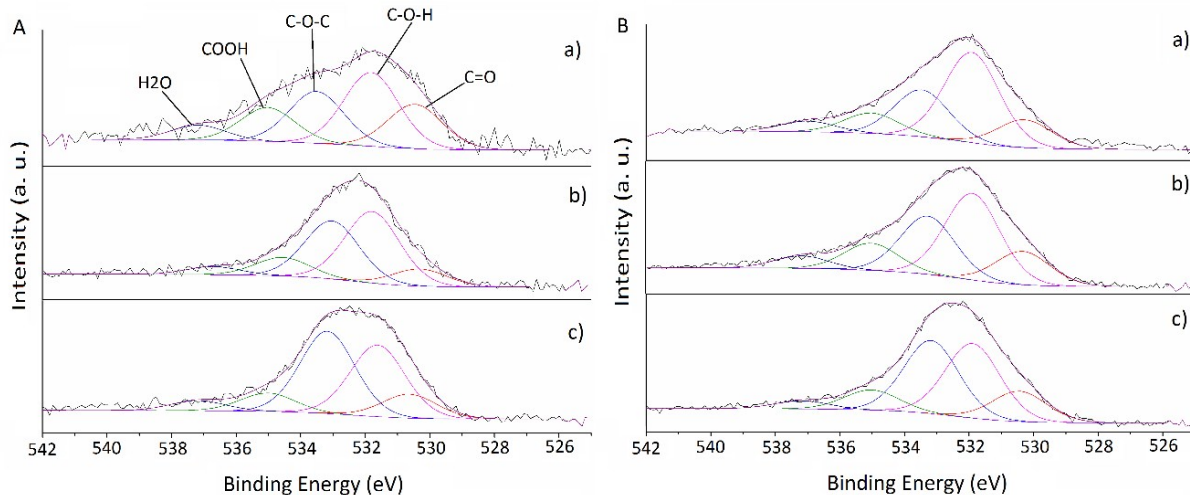


Figure S5. XPS spectra of fresh Pd/CNF in the binding energy region of 525-542 eV corresponding to O1s. (A) Catalyst synthesised by impregnation: (a) Pd_{IMP}/CNF-HHT, (b) Pd_{IMP}/CNF-LHT, (c) Pd_{IMP}/CNF-PS. (B) Catalysts synthesised by sol-immobilisation: (a) Pd_{SI}/CNF-HHT, (b) Pd_{SI}/CNF-LHT, (c) Pd_{SI}/CNF-PS.

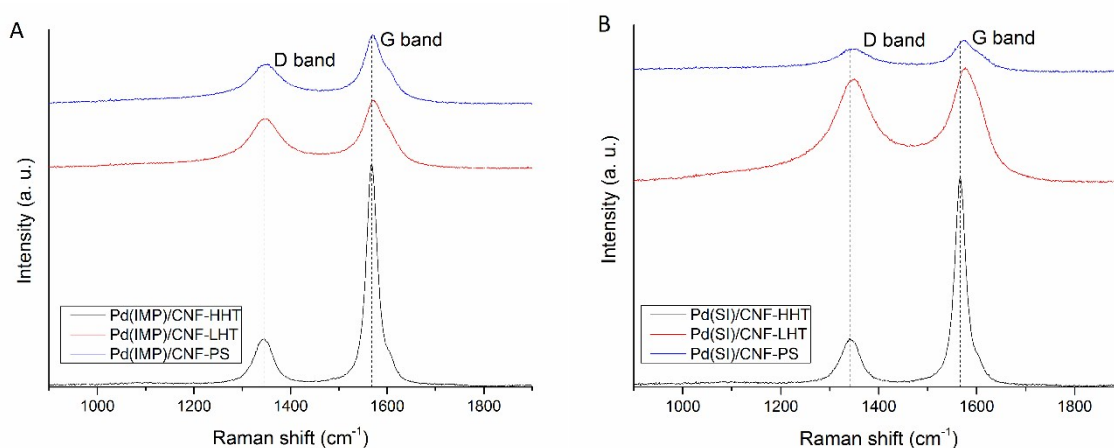


Figure S6. Raman spectra of the used samples. (A) Catalyst synthesised by impregnation: (a) Pd_{IMP}/CNF-HHT (black curve), (b) Pd_{IMP}/CNF-LHT (red curve), (c) Pd_{IMP}/CNF-PS (blue curve). (B) Catalysts synthesised by sol-immobilisation: (a) Pd_{SI}/CNF-HHT (black curve), (b) Pd_{SI}/CNF-LHT (red curve), (c) Pd_{SI}/CNF-PS (blue curve).

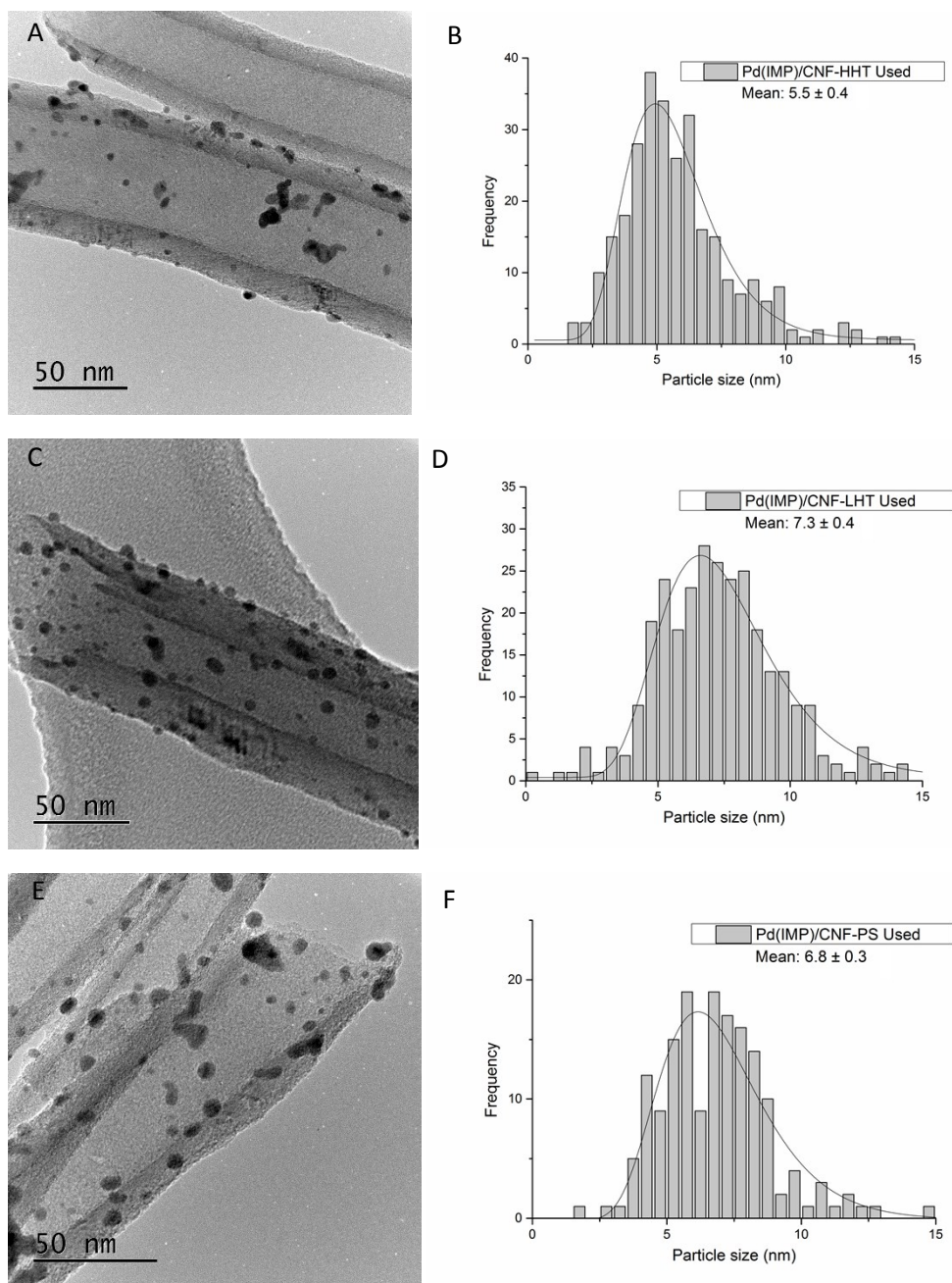


Figure S7. Bright field TEM micrographs and corresponding histograms of the particle size distributions for the used catalysts prepared by impregnation. (A,B) Pd_{IMP}/CNF-HHT, (C,D) Pd_{IMP}/CNF-LHT, (E,F) Pd_{IMP}/CNF-PS.

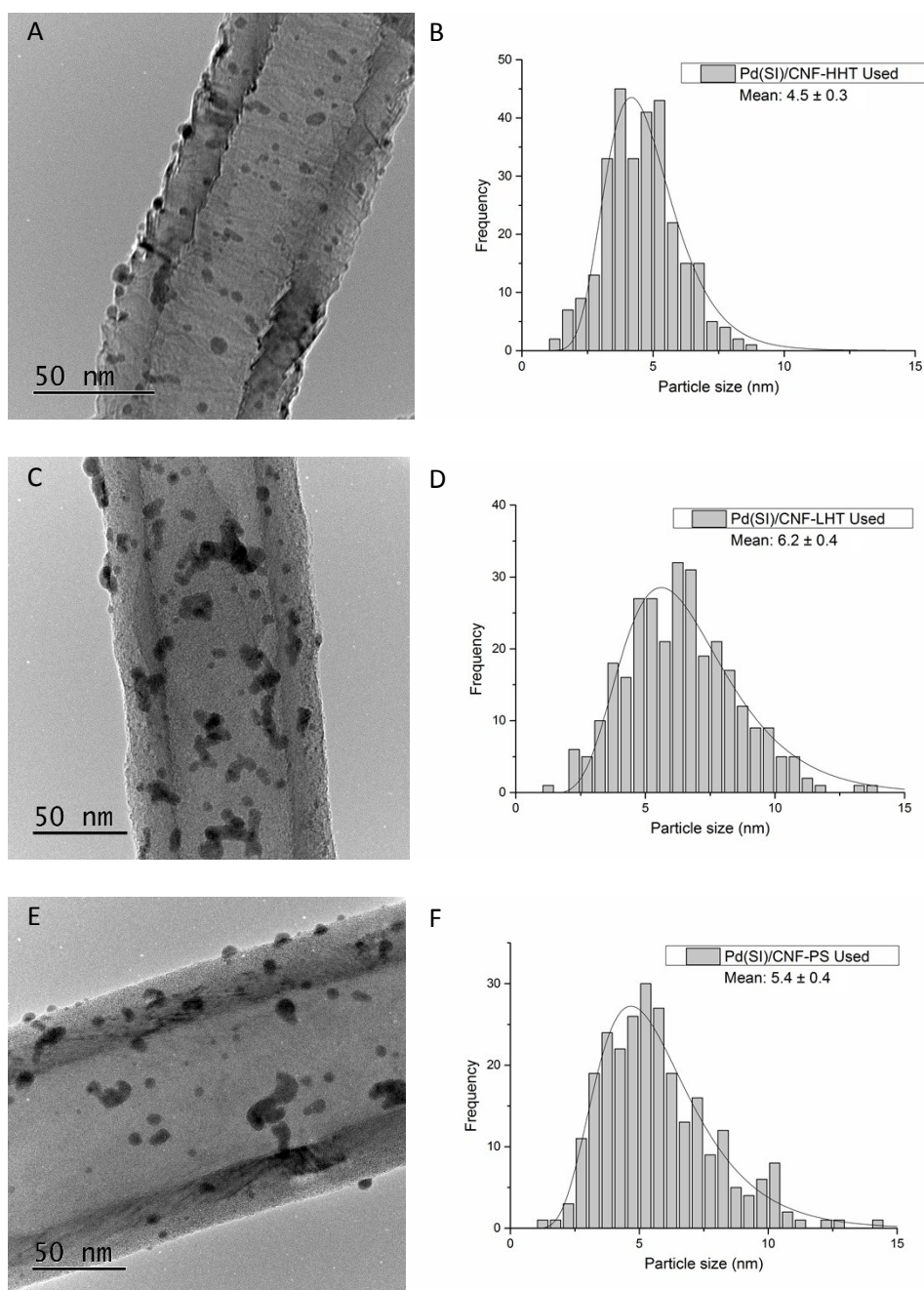


Figure S8. Bright field TEM micrographs and corresponding histograms of the particle size distributions for the used catalysts prepared by sol-immobilisation. (A,B) Pd_{SI}/CNF-HHT, (C,D) Pd_{SI}/CNF-LHT, (E,F) Pd_{SI}/CNF-PS.

| Catalyst | Temp (°C) | H ₂ (%) | CO ₂ (%) | CO (ppm) | CO/CO ₂ |
|----------------------------|-----------|--------------------|---------------------|----------|--------------------|
| Pd _{IMP} /CNF-HHT | 30 | 6.3 | 5.7 | 14.7 | 0.000258 |
| Pd _{SI} /CNF-HHT | 30 | 5.9 | 6.3 | 11.0 | 0.000175 |

Table S1. Concentrations of H₂, CO₂ and CO evolved at 30 °C and ratio CO/CO₂.

